Bulk-edge correspondence for the nonlinear eigenvalues problem of the Haldane model

Shujie Cheng,[1,2,*] Yonghua Jiang,[1,†] and Gao Xianlong[2,‡]
[1]*Xingzhi College, Zhejiang Normal University, Lanxi 321100, China*
[2]*Department of Physics, Zhejiang Normal University, Jinhua 321004, China*

(Received 4 December 2023; revised 1 February 2024; accepted 12 March 2024; published 1 April 2024)

Recently, there is an interest in studying the bulk-edge correspondence for nonlinear eigenvalue problems in a two-dimensional topological system with spin-orbit coupling. By employing the method of the auxiliary eigenvalues as introduced in T. Isobe *et al.*, Phys. Rev. Lett. **132**, 126601 (2024), the nonlinear bulk-edge correspondence was established. In this paper, taking the Haldane model as an example, we address that such a correspondence will appear in two-dimensional topological systems without spin-orbit coupling. The resulting edge states are characterized by the Chern number of the auxiliary energy band. A full phase diagram containing topological nontrivial phase, topological trivial phase, and metallic phase is obtained. Our work generalizes the study of the bulk-edge correspondence for nonlinear eigenvalue problems in two-dimensional systems.

DOI: 10.1103/PhysRevB.109.134201

I. INTRODUCTION

For decades, the novel nature of the topological phase of matter has sparked significant interest among researchers in the field of condense matter topology. Specifically, topological band theory plays a critical role in revealing a variety of topological phases by integrating the energy band theory and the concept of topology [1–12]. One of the most fascinating phenomena in topological systems is the bulk-edge correspondence (BEC), which showcases the appearance of edge states triggered by the bulk topology [13,14]. One can employ the quantum transport to check this correspondence. The topological systems with nonzero quantized topological invariant presents nonzero quantized Hall conductance in the transport measurement [15,16]. Besides, the BEC shows extreme robustness against the disorders [17–32].

Extending the topological band theory to nonlinear systems brings about exotic phenomena as well. Precisely, Refs. [33–41] have recently studied the interaction between topology and nonlinearity of the eigenvectors, clarifying the occurrence of topological synchronization brought about by the interplay between nonlinearity and topology [37]. In spite of extensive efforts made as described above, the interaction between the topology and nonlinear eigenvalues, which represent another form of nonlinearity [42–44], has been seldom investigated. Very recently, Isobe *et al.* studied the BEC for the two-dimensional nonlinear eigenvalue systems with spin-orbit coupling [45]. The nonlinear BEC was established by introducing the auxiliary eigenvalues. The work provides a motivation for us to study whether there are nonlinear eigenvalues of BEC in two-dimensional systems beyond the spin-orbit coupling mechanism. We note that the Haldane model [1] is a topological system without spin-orbit coupling. The predicted nontrivial topological quantum anomalous Hall effect has been experimentally observed [46,47]. The study of nonlinear eigenvalue BEC without spin-orbit coupling is a natural extension of the research work by Isobe *et al.* With the Haldane model as a medium, in this paper we will address the aforementioned issue.

This paper is organized as follows. Section II introduces the nonlinear eigenvalue problem of the Haldane model. Section III presents the numerical results about edge states and phase diagrams, and the analytical phase boundary. Section IV presents our discussions and summary.

II. NONLINEAR EIGENVALUES PROBLEM OF HALDANE MODEL

Here, we take the same strategy as told in Ref. [45], i.e., employing the method of the auxiliary eigenvalues to analyze the nonlinear BEC of the Haldane model. Similarly, we discuss the BEC between the gapless edge states and the auxiliary topological bands by introducing the auxiliary eigenvalues. The nonlinear eigenvalue problem of the Haldane model is established by the following nonlinear equation:

$$H(\mathbf{k})|\psi\rangle = \omega S(\omega,\ \mathbf{k})|\psi\rangle, \tag{1}$$

where $H(\mathbf{k})$ is the Hamiltonian matrix of the Haldane model, $S(\omega,\ \mathbf{k})$ is the overlap matrix, $\mathbf{k}$ is the momentum, $|\psi\rangle$ is the eigenvector, and ω is the nonlinear parameter. $H(\mathbf{k})$ is given by

$$H(\mathbf{k}) = \begin{pmatrix} d_3 & d_1 - id_2 \\ d_1 + id_2 & -d_3 \end{pmatrix}. \tag{2}$$

The Hamiltonian elements d_1, d_2, and d_3 are

$$d_1 = \sum_{n=1,2,3} t_1 \cos(\mathbf{k}\cdot a_n),$$

$$d_2 = \sum_{n=1,2,3} t_1 \sin(\mathbf{k}\cdot a_n),$$

$$d_3 = M - \sum_{n=1,2,3} 2t_2 \sin(\varphi)\sin(\mathbf{k}\cdot b_n),$$

*chengsj@zjnu.edu.cn
†yonghua_j82@zjnu.cn
‡gaoxl@zjnu.edu.cn

where t_1 is the unit of energy and

$$a_1 = \begin{pmatrix} 0 \\ -1 \end{pmatrix},\ a_2 = \begin{pmatrix} \frac{\sqrt{3}}{2} \\ \frac{1}{2} \end{pmatrix},\ a_3 = \begin{pmatrix} -\frac{\sqrt{3}}{2} \\ \frac{1}{2} \end{pmatrix},$$
$$b_1 = \begin{pmatrix} \sqrt{3} \\ 0 \end{pmatrix},\ b_2 = \begin{pmatrix} -\frac{\sqrt{3}}{2} \\ \frac{3}{2} \end{pmatrix},\ b_3 = \begin{pmatrix} -\frac{\sqrt{3}}{2} \\ -\frac{3}{2} \end{pmatrix} \quad (3)$$

are lattice vectors, $t_2e^{i\varphi}$ is the hopping strength between two same type sites, and M is the strength of on-site potential.

In fact, solving Eq. (1) is equivalent to solving $P(\omega,\ \mathbf{k})|\psi\rangle = 0$, where $P(\omega,\ \mathbf{k}) = H(\mathbf{k}) - \omega S(\omega,\ \mathbf{k})$ [43]. To analyze the BEC of Eq. (1), it is helpful to introduce the auxiliary eigenvalues λ, and the nonlinear eigenvalue problem becomes

$$P(\omega,\ \mathbf{k})|\psi\rangle = \lambda|\psi\rangle. \quad (4)$$

We shall remember that λ is an auxiliary quantity that only has physical meaning at $\lambda = 0$. Therefore, the above eigenvalue problem is transformed into finding the solution of $\lambda = 0$.

In Ref. [45], in establishing the above analysis process, the authors made an existence assumption of $\lambda = 0$, such that one can observe the emergence and disappearance of gapless edge states at $\lambda = 0$. For the nonlinear eigenvalue problem of the Haldane model, we argue that the assumption of $\lambda = 0$ is valid as well. At first, the energy spectrum of the Haldane model presents inversion symmetry. We consider a grip geometry of the Haldane lattice [see sketch in Fig. 1(a)], leaving a periodic boundary condition in the x direction and open boundary condition in the y direction (armchair edge). Hence, the lattice constant is $3a$. The armchair edge spectrum $E(k_x)$ as a function of the momentum k_x is plotted in Fig. 1(b). Here, the spectrum $E(k_x)$ is obtained from $H(\mathbf{k})$. As seen that the spectrum is symmetric with respect to $E(k_x) = 0$, presenting the inversion symmetry, and the edge states inevitably cross $E(k_x) = 0$. Second, we choose an overlap matrix S only depending on the nonlinear parameter ω, which is given by

$$S(\omega) = \begin{pmatrix} 1 - M_s(\omega) & 0 \\ 0 & 1 + M_s(\omega) \end{pmatrix}, \quad (5)$$

where $M_s(\omega) = M_1 \tanh(\omega)/\omega$. The overlap matrix multiplying $-\omega$, i.e., the nonlinear term $-\omega S(\omega)$ here, acts as the chemical potentials dependent on the sites and the parameter ω. For R sites, the chemical potentials are $-\omega + \omega M_s(\omega)$, and for B sites, the chemical potentials are $-\omega - \omega M_s(\omega)$. To study the topological properties of such systems with sites and parameter dependent chemical potentials, we can establish the nonlinear eigenvalue equation as shown in Eq. (1) and introduce the auxiliary eigenvalues. Therefore, the eigenvalue problems of such systems naturally become nonlinear eigenvalue problems. From the expression of $\omega \pm \omega M_s(\omega)$, we know that they are monotonic with the change of ω. When the nonlinearity is weak, i.e., ω is small, the eigenvalues of $S(\omega)$ are slow varying with respect to ω. Therefore, the up and down translation of the λ spectrum caused by the nonlinear effect is small, and we can observe the physical edge states at $\lambda = 0$. In addition, the choice of $S(\omega)$ has been proved to be feasible to establish the nonlinear BEC in Ref. [45]. If $\omega = 0$, there is no nonlinear effect, and Eq. (1) is reduced to an ordinary eigenvalue problem. We know that there is a topological nontrivial-trivial transition in the ordinary eigenvalue problem of the Haldane model [1]. In the following, without loss of generality, we fix the parameters $t_2 = M_1 \equiv t_1$ and $\varphi = \pi/2$ to analyze the nonlinear BEC of the Haldane model, and explore the phenomena caused by the nonlinear effect.

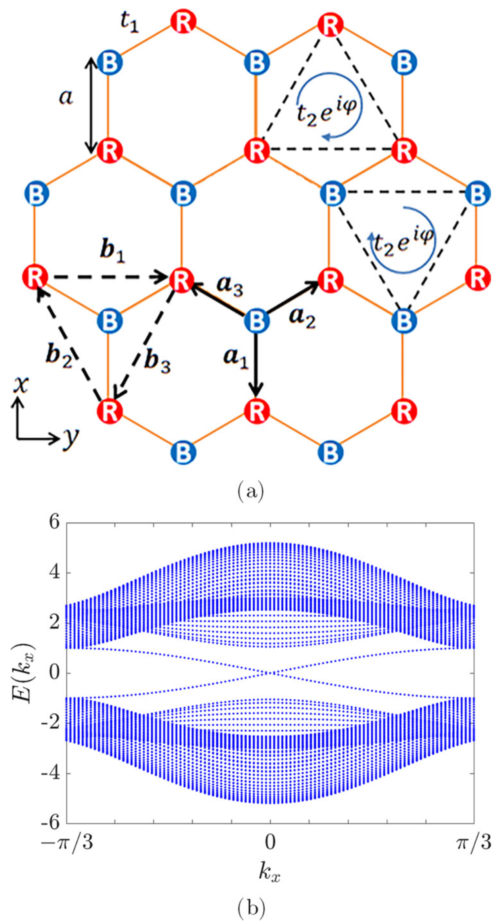

FIG. 1. (a) Sketch of the Haldane lattice. R and B are two types of sublattice sites. $\boldsymbol{a}_{n=1,2,3}$ and $\boldsymbol{b}_{n=1,2,3}$ are lattice vectors. The bond length is set as $a = 1$. t_1 is the hopping strength between nearest-neighbor sites (set as the unit of energy), and $t_2e^{-i\varphi}$ is the hopping strength between two same type sites. The on-site potential at the R site is M and the one at the B site is $-M$. (b) Armchair edge energy spectrum of the Haldane under $t_2 = t_1$, $\varphi = \pi/2$, and $M = 0$. Here, the spectrum $E(k_x)$ is obtained from $H(\mathbf{k})$.

III. NONLINEAR BULK-EDGE CORRESPONDENCE

We start by analyzing the auxiliary λ spectrum under different M. Similarly, the λ spectra in the following are plotted by selecting a strip geometry with armchair edge in the y direction. To plot λ-ω spectra, we choose $k_x = 0$ as an example. Under $M = 2t_1$, the corresponding λ spectrum as a function of the nonlinear parameter ω is plotted in Fig. 2(a). As seen, there are edge states crossing $\lambda = 0$ under moderate values of ω. To see the edge state clearly, we plot the λ as a function of k_x under $M = 2t_1$ and $\omega = 0.5$ in Fig. 2(d). Intuitively, $\lambda = 0$ is within the bulk gap in the λ spectrum and there are a pair of edge states at $\lambda = 0$, presenting nontrivial

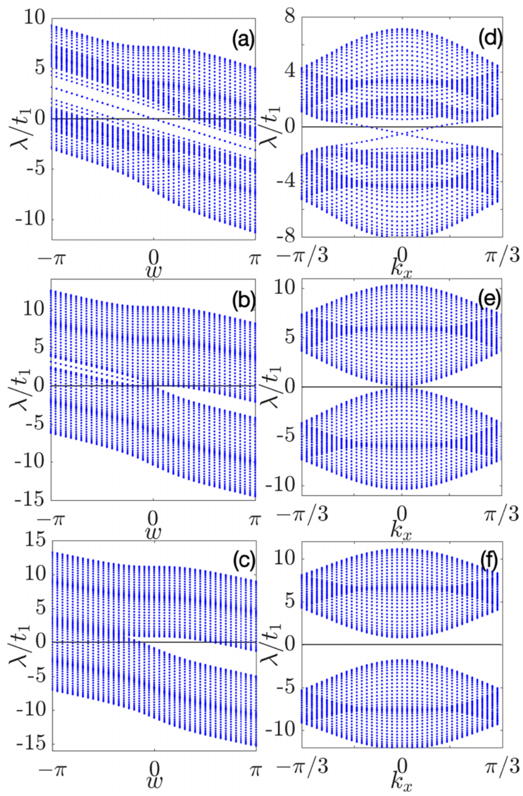

FIG. 2. Auxiliary λ spectrum of the Haldane model, shown with blue dots. The horizontal black lines are reference lines at $\lambda = 0$. (a)–(c) present λ-ω spectra under $k_x = 0$ with $M = 2t_1$, $M = 3\sqrt{3}t_1$, and $M = 6t_1$, respectively. (d)–(f) present λ-k_x spectra under $\omega = 0.5$, $\omega = 0$, and $\omega = 0.5$, respectively.

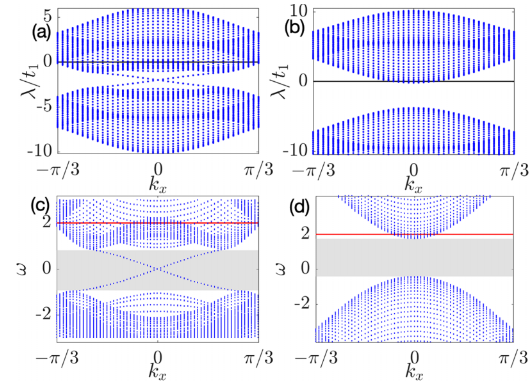

FIG. 3. (a) and (b): Armchair edge λ spectra under $\omega = 2$ with $M = 2t_1$ in (a) and $M = 6t_1$ in (b), respectively. The horizontal black lines are the $\lambda = 0$ reference lines. (c) and (d): Band structures of ω versus k_x extracted from $\lambda = 0$ with $M = 2t_1$ in (a) and $M = 6t_1$ in (b), respectively. The gray regions show the band gaps. The horizontal red lines are the $\omega = 2$ reference lines.

topological property. With $M = 3\sqrt{3}t_2$, the λ spectrum versus ω is presented in Fig. 2(b). We can see that the bands of $\lambda = 0$ close at $\omega = 0$. Equivalently, the bands in the λ spectrum touch at $\lambda = 0$ and $k_x = 0$ [see Fig. 2(e) for details]. For larger M, such as $M = 6t_1$, we plot the λ spectrum with respect to ω in Fig. 2(c). It shows that there is no edge state because $\lambda = 0$ is within a distinct gap of the λ spectrum, presenting trivial topological property. Similarly, we can see the feature in the λ-k_x spectrum as well. As Fig. 2(f) shows, $\lambda = 0$ is within the band gap of the auxiliary λ spectrum, but no edge state crosses it.

According to conventional principle of bulk-edge correspondence [13,14], the emergence of edge states can be forecasted by the energy band Chern number, and the magnitude of the Chern number counts the number of the paired edge states. Next, we check the correspondence between the Chern number of the bulk band of λ and the emergent edge states at $\lambda = 0$. The Chern number of the band in the auxiliary λ spectrum below $\lambda = 0$, namely $C_1(\omega)$, is defined as

$$C_1(\omega) = \frac{1}{2\pi} \oint_{\partial_{IBZ}} \boldsymbol{A}_1(\mathbf{k}, \omega)\, d\mathbf{k}, \tag{6}$$

where ∂_{IBZ} means the boundary of the first Brillouin zone, and $\boldsymbol{A}_1(\mathbf{k}, \omega) = -i\langle\psi_1(\mathbf{k}, \omega)|\nabla_{\mathbf{k}}|\psi_1(\mathbf{k}, \omega)\rangle$ with $|\psi_1(\mathbf{k}, \omega)\rangle$ being the corresponding eigenvector. If a topological system has more than two bands, multiple auxiliary bands may appear below $\lambda = 0$. In this case, one needs to calculate the sum of the Chern numbers of the auxiliary bands to characterize the topological phases. For the two-band system, there is only one band below $\lambda = 0$. Therefore, it is enough to use $C_1(\omega)$ to characterize the topological phases. We analytically and numerically calculate $C_1(\omega = 2)$ of the band below $\lambda = 0$ in Fig. 2(d) and Fig. 2(f), and find $C_1 = 1$ and $C_1 = 0$, respectively. Here the analytical C_1 can be available by the singularity expansion method [48,49]. It means that the correspondence between the number of paired edge states and the Chern number of the band below $\lambda = 0$ is valid in the nonlinear eigenvalue problem of the Haldane model.

What we have discussed before are the cases where ω are relatively small, and we find that when ω is relatively large, the system will enter the metallic phase, which can not be characterized by the Chern number of the auxiliary energy band. We note that in Ref. [45], the authors have studied the BEC for the two-dimensional and three-dimensional nonlinear eigenvalue systems with spin-orbit coupling, and the corresponding phase diagrams show that there is no metallic phase in such systems. Here, the underlying metallic phase in our nonlinear eigenvalue system without spin-orbit coupling is an obvious difference from their findings. Taking $\omega = 2$ and $M = 2t_1$ as an example, we plot the λ spectrum as a function of k_x under the armchair edge in Fig. 3(a). As can be seen, the states at $\lambda = 0$ have been embeded into the bulk of the system (see the horizontal black reference lines). We name this state the metallic phase. The metallic phase appears invthe $C_1 = 0$ case as well. Considering $\omega = 2$ and $M = 6t_1$, we plot the corresponding λ spectrum in Fig. 3(b). It is seen that the states at $\lambda = 0$ are embeded into the bulk of the system. Moreover, this metallic characteristic can be observed in the ω-k_x spectrum as well. Figure 3(c) presents the band structure of ω as the varying of k_x under $M = 2t_1$. The data are extracted from $\lambda = 0$. As it shows, the edge states only exist in small regions of the nonlinear parameter ω [the shadow region in Fig. 3(c)] where there are bulk energy gaps, and the presence of the edge state can be interpreted by $C_1 = 1$. It means that there exists nonlinear BEC between the

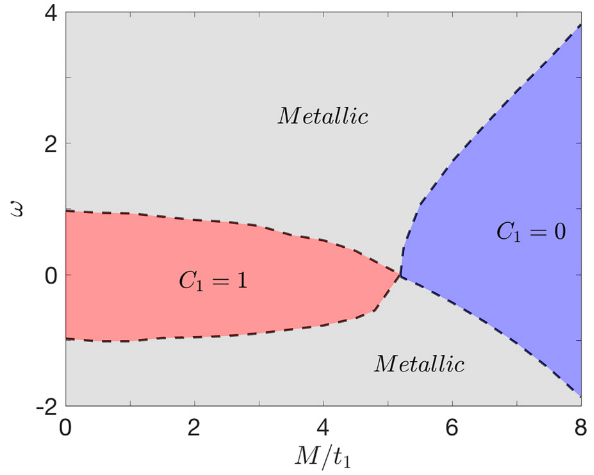

FIG. 4. Phase diagram of the nonlinear Haldane model. The red region denotes the topological nontrivial phase with $C_1 = 1$. The blue region denotes the topological trivial phase with $C_1 = 0$. The gray region denotes the metallic phase.

ω-k_x spectrum and the energy band Chern number as well. For strong nonlinearity, there is no edge state but bulk states (see the $\omega = 2$ horizontal red line for example), showing the metallic feature of the system. In addition, similar nonlinear BEC and metallic characteristic can be seen in the $M = 6t_1$ case as well. We plot the corresponding band structure of ω as a function of k_x in Fig. 3(d). The data are still extracted from $\lambda = 0$. Intuitively, there exists nonlinear BEC. When ω is small, there is a bulk energy gap [the shadow region in Fig. 3(d)], and the absence of an edge state can be interpreted by $C_1 = 0$. For strong nonlinearity, such $\omega = 2$ (the horizontal red reference line), the corresponding states are embed into the bulk of the system, presenting the metallic property.

By analyzing the band structures of the λ and ω spectra under more discrete parameter points, the phase of the nonlinear Haldane model is plotted in the ω-M parameter space, which is shown in Fig. 4. We determine that the nonlinear system contains three phases: the topological nontrivial phase with $C_1 = 1$ (red region), the topological trivial phase with $C_1 = 0$ (blue region), and the metallic phase (gray region). The black dashed lines are the phase boundaries between the metallic phase and the topological phases. From the phase diagram, we can intuitively see that the topological nontrivial phase is more sensitive to the nonlinearity compared to the topological trivial phase. The topological nontrivial phase only exists in the cases where the nonlinear parameters ω are weak (less than one), while the trivial phase can survive in the cases where ω are strong (far larger than one). When the nonlinear parameter ω is fixed at a finite nonzero value, as the increase of the on-site potential strength, the system can undergo the transition from the $C_1 = 1$ phase to the metallic phase, and finally to the $C_1 = 0$ phase. It is also feasible to continuously tune both the nonlinear parameters and the strength of the potential, achieving a direct transition from $C_1 = 1$ to $C_1 = 0$ without experiencing the metallic phase.

The metallic phase, topological nontrivial phase, and the topological trivial phase can be detected by the transport conductance G as well. According to the Landauer formula

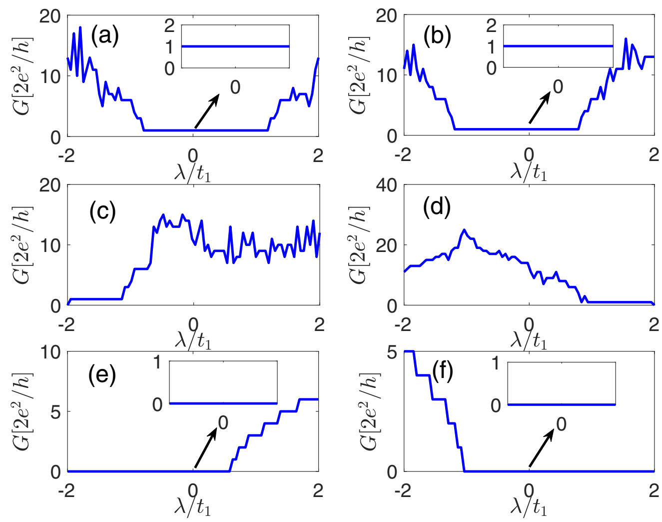

FIG. 5. Transport conductance G as a function of the auxiliary eigenvalue λ. (a) $M = 2t_1$ and $\omega = 0.2$; (b) $M = 2t_1$ and $\omega = -0.2$; (c) $M = 2t_1$ and $\omega = 2$; (d) $M = 2t_1$ and $\omega = -2$; (e) $M = 6t_1$ and $\omega = 1$; (f) $M = 8t_1$ and $\omega = -1$. The insets enlarge the transport conductance near $\lambda = 0$.

[50,51], G is obtained from

$$G = \frac{2e^2}{h} T_\lambda, \tag{7}$$

where T_λ is the transmission coefficient and $2e^2/h$ is the unit of G. Taking different M and ω, we plot the corresponding transport conductance G as a function of the auxiliary eigenvalue λ in Figs. 5(a)–5(f). Specifically, Figs. 5(a) and 5(b) show that there are quantized conductance $G = 2e^2/h$ at $\lambda = 0$, presenting the topological nontrivial feature. In Figs. 5(c) and 5(d), the curves show that there are macroscopic nonquantized conductance at $\lambda = 0$, revealing the metallic property of the nonlinear Haldane model under the current parameters. In Figs. 5(e) and 5(f), there are quantized transport conductances at $\lambda = 0$ as well, but $G = 0$, which reflects the topological trivial property of the system under the current parameters. The results of the transport conductance are self-consistent with our phase diagram. Although we only select six sets of parameters to analyze the transport conductance, for other parameters, the results are self-consistent with our phase diagram as well.

IV. SUMMARY

Herein, we have studied the nonlinear eigenvalue problem of the Haldane model in the absence of spin-orbit coupling. Similar to Ref. [45], we find that there is nonlinear bulk-edge correspondence as well. Meanwhile, when the nonlinearity is within a threshold, the emergence and disappearance of the edge states can be characterized by the Chern number of the auxiliary energy band as well, but differently, we find that when the nonlinearity exceeds the threshold, this nonlinear system will enter the metallic phase, which has no analog in the Haldane model and the two-dimensional and three-dimensional nonlinear eigenvalue systems with spin-orbit coupling [45] as well. Compared to the topological trivial phase, the topological non-trivial phase is more fragile to the nonlinearity, because it only appears in the cases where the nonlinearity is relative weak. Our work enriches the study of the bulk-edge correspondence of nonlinear eigenvalues of two-dimensional systems. Noting that the Haldane model has been experimentally realized [47], we expect that nonlinear bulk-edge correspondence of the Haldane model can be observed on similar experimental platforms in the near future.

ACKNOWLEDGMENT

We acknowledge support from the NSFC under Grants No. 12174346 and No. 51405449.

[1] F. D. M. Haldane, Model for a quantum Hall effect without landau levels: Condensed-matter realization of the "parity anomaly", Phys. Rev. Lett. **61**, 2015 (1988).
[2] C. L. Kane and E. J. Mele, Quantum spin Hall effect in graphene, Phys. Rev. Lett. **95**, 226801 (2005).
[3] L. Fu, C. L. Kane, and E. J. Mele, Topological insulators in three dimensions, Phys. Rev. Lett. **98**, 106803 (2007).
[4] M. Z. Hasan and C. L. Kane, *Colloquium:* Topological insulators, Rev. Mod. Phys. **82**, 3045 (2010).
[5] X.-L. Qi and S.-C. Zhang, Topological insulators and superconductors, Rev. Mod. Phys. **83**, 1057 (2011).
[6] Y. Ando, Topological insulator materials, J. Phys. Soc. Jpn. **82**, 102001 (2013).
[7] C.-K. Chiu, J. C. Y. Teo, A. P. Schnyder, and S. Ryu, Classification of topological quantum matter with symmetries, Rev. Mod. Phys. **88**, 035005 (2016).
[8] A. P. Schnyder, S. Ryu, A. Furusaki, and A. W. W. Ludwig, Classification of topological insulators and superconductors in three spatial dimensions, Phys. Rev. B **78**, 195125 (2008).
[9] A. Kitaev, Periodic table for topological insulators and superconductors, in *AIP Conference Proceedings* (American Institute of Physics, Maryland, USA, 2009), Vol. 1134, pp. 22–30.
[10] S. Ryu, A. P. Schnyder, A. Furusaki, and A. W. W. Ludwig, Topological insulators and superconductors: tenfold way and dimensional hierarchy, New J. Phys. **12**, 065010 (2010).
[11] N. Nagaosa, J. Sinova, S. Onoda, A. H. MacDonald, and N. P. Ong, Anomalous Hall effect, Rev. Mod. Phys. **82**, 1539 (2010).
[12] D. Xiao, M.-C. Chang, and Q. Niu, Berry phase effects on electronic properties, Rev. Mod. Phys. **82**, 1959 (2010).
[13] Y. Hatsugai, Chern number and edge states in the integer quantum Hall effect, Phys. Rev. Lett. **71**, 3697 (1993).
[14] Y. Hatsugai, Edge states in the integer quantum Hall effect and the riemann surface of the Bloch function, Phys. Rev. B **48**, 11851 (1993).
[15] C.-Z. Chang, J. Zhang, X. Feng, J. Shen, Z. Zhang, M. Guo, K. Li, Y. Ou, P. Wei, L.-L. Wang, Z.-Q. Ji, Y. Feng, S. Li, X. Chen, J. Jia, X. Dai, Z. Fang, S.-C. Zhang, K. He, Y. Wang, L. Lu, X.-C. Ma, and Q.-K. Xue, Experimental observation of the quantum anomalous Hall effect in a magnetic topological insulator, Science **340**, 167 (2013).
[16] M. Z. Shi, Z. Guo, Z. Xu, J. Wang, X. H. Chen, Y. Deng, Y. Yu, and Y. Zhang, Quantum anomalous Hall effect in intrinsic magnetic topological insulator $MnBi_2Te_4$, Science **367**, 895 (2020).
[17] E. Prodan, T. L. Hughes, and B. A. Bernevig, Entanglement spectrum of a disordered topological Chern insulator, Phys. Rev. Lett. **105**, 115501 (2010).
[18] E. Prodan, Disordered topological insulators: a non-commutative geometry perspective, J. Phys. A: Math. Theor. **44**, 113001 (2011).
[19] Z. Xu, L. Sheng, D. Y. Xing, E. Prodan, and D. N. Sheng, Topologically protected extended states in disordered quantum spin-Hall systems without time-reversal symmetry, Phys. Rev. B **85**, 075115 (2012).
[20] M. Gonçalves, P. Ribeiro, and E. V. Castro, The haldane model under quenched disorder, arXiv:1807.11247.
[21] H. Li, C.-Z. Chen, H. Jiang, and X. C. Xie, Coexistence of quantum Hall and quantum anomalous Hall phases in disordered $MnBi_2Te_4$, Phys. Rev. Lett. **127**, 236402 (2021).
[22] D. D. Vu and S. Das Sarma, Weak quantization of noninteracting topological Anderson insulator, Phys. Rev. B **106**, 134201 (2022).
[23] J. Li, R.-L. Chu, J. K. Jain, and S.-Q. Shen, Topological Anderson insulator, Phys. Rev. Lett. **102**, 136806 (2009).
[24] H. Jiang, L. Wang, Q.-F. Sun, and X. C. Xie, Numerical study of the topological Anderson insulator in HgTe/CdTe quantum wells, Phys. Rev. B **80**, 165316 (2009).
[25] C. W. Groth, M. Wimmer, A. R. Akhmerov, J. Tworzydło, and C. W. J. Beenakker, Theory of the topological Anderson insulator, Phys. Rev. Lett. **103**, 196805 (2009).
[26] C. P. Orth, T. Sekera, C. Bruder, and T. L. Schmidt, The topological Anderson insulator phase in the Kane-Mele model, Sci. Rep. **6**, 24007 (2016).
[27] J. Song, H. Liu, H. Jiang, Q.-F. Sun, and X. C. Xie, Dependence of topological Anderson insulator on the type of disorder, Phys. Rev. B **85**, 195125 (2012).
[28] J. H. García, L. Covaci, and T. G. Rappoport, Real-space calculation of the conductivity tensor for disordered topological matter, Phys. Rev. Lett. **114**, 116602 (2015).
[29] Y.-Y. Zhang, R.-L. Chu, F.-C. Zhang, and S.-Q. Shen, Localization and mobility gap in the topological Anderson insulator, Phys. Rev. B **85**, 035107 (2012).
[30] Y. Fu, J. H. Wilson, and J. H. Pixley, Flat topological bands and eigenstate criticality in a quasiperiodic insulator, Phys. Rev. B **104**, L041106 (2021).
[31] M. F. Madeira and P. D. Sacramento, Quasidisorder-induced topology, Phys. Rev. B **106**, 224505 (2022).
[32] Y.-P. Wu, L.-Z. Tang, G.-Q. Zhang, and D.-W. Zhang, Quantized topological Anderson-thouless pump, Phys. Rev. A **106**, L051301 (2022).
[33] V. Goblot, B. Rauer, F. Vicentini, A. Le Boité, E. Galopin, A. Lemaître, L. Le Gratiet, A. Harouri, I. Sagnes, S. Ravets, C. Ciuti, A. Amo, and J. Bloch, Nonlinear polariton fluids in a flatband reveal discrete gap solitons, Phys. Rev. Lett. **123**, 113901 (2019).
[34] M. Ezawa, Nonlinearity-induced chiral solitonlike edge states in Chern systems, Phys. Rev. B **106**, 195423 (2022).

[35] M. Ezawa, Nonlinear topological phase transitions in the dimerized sine-Gordon model, Phys. Rev. B **105**, 165418 (2022).
[36] M. Ezawa, Topological edge states and bulk-edge correspondence in dimerized Toda lattice, J. Phys. Soc. Jpn. **91**, 024703 (2022).
[37] K. Sone, Y. Ashida, and T. Sagawa, Topological synchronization of coupled nonlinear oscillators, Phys. Rev. Res. **4**, 023211 (2022).
[38] N. Pernet, P. St-Jean, D. D. Solnyshkov, G. Malpuech, N. Carlon Zambon, Q. Fontaine, B. Real, O. Jamadi, A. Lemaitre, M. Morassi, L. L. Gratiet, T. Baptiste, A. Harouri, I. Sagnes, A. Amo, S. Ravets, and J. Bloch, Gap solitons in a one-dimensional driven-dissipative topological lattice, Nat. Phys. **18**, 678 (2022).
[39] L. Jezequel and P. Delplace, Nonlinear edge modes from topological one-dimensional lattices, Phys. Rev. B **105**, 035410 (2022).
[40] K. Sato and T. Fukui, Chern numbers associated with the periodic Toda lattice, J. Phys. Soc. Jpn. **92**, 073001 (2023).
[41] K. Sone, M. Ezawa, Y. Ashida, N. Yoshioka, T. Sagawa, Nonlinearity-induced topological phase transition characterized by the nonlinear Chern number, arXiv:2307.16827.
[42] V. Kuzmiak, A. A. Maradudin, and F. Pincemin, Photonic band structures of two-dimensional systems containing metallic components, Phys. Rev. B **50**, 16835 (1994).
[43] S. Raghu and F. D. M. Haldane, Analogs of quantum-Hall-effect edge states in photonic crystals, Phys. Rev. A **78**, 033834 (2008).
[44] H. H. Huang, C. T. Sun, and G. L. Huang, On the negative effective mass density in acoustic metamaterials, Int. J. Eng. Sci. **47**, 610 (2009).
[45] T. Isobe, T. Yoshida, and Y. Hatsugai, Bulk-edge correspondence for nonlinear eigenvalue problems, Phys. Rev. Lett. **132**, 126601 (2024).
[46] M. Aidelsburger, M. Lohse, C. Schweizer, M. Atala, J. T. Barreiro, S. Nascimbene, N. Cooper, I. Bloch, and N. Goldman, Measuring the Chern number of Hofstadter bands with ultracold bosonic atoms, Nat. Phys. **11**, 162 (2015).
[47] G. Jotzu, M. Messer, R. Desbuquois, M. Lebrat, T. Uehlinger, D. Greif, and T. Esslinger, Experimental realization of the topological haldane model with ultracold fermions, Nature (London) **515**, 237 (2014).
[48] T. Andrijauskas, E. Anisimovas, M. Račiūnas, A. Mekys, V. Kudriašov, I. B. Spielman, and G. Juzeliūnas, Three-level Haldane-like model on a dice optical lattice, Phys. Rev. A **92**, 033617 (2015).
[49] P. Wang, M. Schmitt, and S. Kehrein, Universal nonanalytic behavior of the Hall conductance in a Chern insulator at the topologically driven nonequilibrium phase transition, Phys. Rev. B **93**, 085134 (2016).
[50] Y. Imry and R. Landauer, Conductance viewed as transmission, Rev. Mod. Phys. **71**, S306 (1999).
[51] S. Datta, *Electronic Transport in Mesoscopic Systems*, Cambridge Studies in Semiconductor Physics and Microelectronic Engineering (Cambridge University Press, Cambridge, UK, 1995).